



 Cite this: *RSC Adv.*, 2024, 14, 15499

# Preparation of carbon quantum dots and their application in the detection of vitamin B2

 Lifen Meng \*<sup>a</sup> and Haizhi Wu<sup>b</sup>

A novel metal-doped carbon quantum dot, zinc-chlorine co-doped carbon quantum dots (Zn/Cl-CQDs), has been developed for the fluorescent probe detection of vitamin B2 and the analysis of the correlation properties of this carbon quantum dot and vitamin B2. Stability experiments demonstrate that Zn/Cl-CQDs possess good fluorescence properties under alkaline conditions. However, when vitamin B2 is added into Zn/Cl-CQDs, the fluorescence intensity decreases sharply, indicating that the fluorescence sensor shows rapid and sensitive detection of vitamin B2 under the static quenching. Lastly, the use of Zn/Cl-CQDs in the detection of vitamin B2 tablets and vitamin B2-rich fruits resulted in recovery rates of 98.2% and 100.6%, respectively. Therefore, this method can be well applied to the detection and analysis of vitamin B2, and has great development prospects in the pharmaceutical industry and food monitoring fields.

 Received 23rd February 2024  
 Accepted 4th May 2024

DOI: 10.1039/d4ra01388c

[rsc.li/rsc-advances](https://rsc.li/rsc-advances)

## 1. Introduction

Fluorescent probes, also known as fluorescent sensors in the field of detection, are fluorescent substances with characteristic fluorescence properties in the ultraviolet-visible-near infrared region, which change with the environment, and changes in fluorescence intensity or wavelength shift.<sup>1–3</sup>

Vitamin B2, also known as riboflavin, is an important water-soluble vitamin that plays a significant role in human health.<sup>4</sup> Vitamin B2 cannot be synthesized in the human body and needs to be obtained from food. The main function of vitamin B2 in the body is to participate in the process of energy metabolism, promoting the metabolism of proteins, fats, and carbohydrates, and maintaining healthy skin, eyes, and the nervous system. Vitamin B2 also has antioxidant properties, as it can eliminate free radicals and protect cells from oxidative damage. Additionally, it promotes the production of red blood cells and maintains normal growth, development, and immune function. Therefore, vitamin B2 is essential for the human body, and since riboflavin cannot be produced by the body itself, it can only be obtained from food or dietary supplements. Hence, the determination of the vitamin content in the human body and various foods is crucial for ensuring human health.<sup>5–9</sup>

However, traditional detection methods have problems such as complex operations, long detection times, and high costs.<sup>10–12</sup> Therefore, developing a simple, rapid, and sensitive method for the detection of vitamin B2 has significant research and

application value. As a new type of fluorescent probe, carbon quantum dots (CQDs), due to their excellent biocompatibility and fluorescence properties, have been widely used in the preparation of biosensors and in bioanalysis.<sup>13–16</sup> This article will focus on the preparation methods of carbon quantum dots and analyze the related properties of carbon dots and their application in the detection of vitamin B2.

The preparation methods of carbon quantum dots are diverse, including hydrothermal method, arc discharge method, laser ablation method, electrochemical oxidation method, microwave method, *etc.*<sup>17,18</sup> Among them, the hydrothermal method is a simple, low-cost, and easy-to-control method, which refers to a method of preparing carbon quantum dots with excellent fluorescence properties by dissolving the preparation materials in water, placing them in a reaction kettle, and reacting under high temperature and high pressure.<sup>19–24</sup> In the detection of vitamin B2, the fluorescent properties of carbon quantum dots are widely used. By reacting carbon quantum dots with vitamin B2, the fluorescence intensity of carbon quantum dots can change, thus achieving the detection of vitamin B2. Studies have shown that using carbon quantum dots as fluorescent probes to detect vitamin B2 is rapid, sensitive, and accurate, and can be used for vitamin B2 detection in the fields of food and medicine. In summary, carbon quantum dots are a new type of nanomaterial with broad application prospects, various preparation methods, and wide application fields. In the detection of vitamin B2, carbon quantum dots as a new type of fluorescent probe have important research value and application prospects.

In recent years, the development of metal-doped carbon quantum dots has attracted widespread attention and has become an effective strategy for adjusting their surface

<sup>a</sup>School of Chemical Engineering, Guizhou University of Engineering Science, 551700, Bijie, China. E-mail: 1025588702@qq.com

<sup>b</sup>School of Mining Engineering, Guizhou University of Engineering Science, Bijie 551700, China



chemical reactivity and electronic properties in many applications such as separation science and analytical detection. So far, there have been some reports on the catalytic properties of metal-doped carbon quantum dots.<sup>25–28</sup> Guo *et al.*<sup>29</sup> successfully synthesized nitrogen-doped carbon quantum dots with citric acid as the carbon source and diethylenetriamine as the nitrogen source using the hydrothermal method. This doped carbon quantum dot emits blue fluorescence, and its quantum yield reaches 84.79%. It has been successfully applied to the detection of tannic acid, proving its huge potential in the field of analytical detection. Preethi, M. *et al.*<sup>30</sup> generates nitrogen-doped carbon quantum dots in one phase by using potato starch as carbon source and ethylenediamine as nitrogen source, a considerable quantum yield (QY) of 49.26% and exhibits a blue fluorescence is observed in the prepared N-CQDs. Under optimum conditions, vitamin C can be added to N-CQDs may promote aggregation and electron transfer due to the interaction between the hydrogen bonds in the N-CQDs and the VC, which may result in fluorescence quenching. As a new material in carbon nanomaterials, it provides new research methods for various related fields, and stands out due to its unique optical properties, and will have huge potential in the field of future detection.

Therefore, in this experiment, the principle of fluorescence quenching is utilized to detect vitamin B2. When vitamin B2 undergoes fluorescence quenching with carbon dots, the fluorescence intensity of CQDs is inversely proportional to the concentration of vitamin B2. Based on the linear relationship, the concentration of vitamin B2 can be easily determined using standard curve.

## 2. Experimental section

### 2.1 Reagents and instruments

**2.1.1 Reagents and materials.** Vitamin B2 standard, zinc gluconate granules, hydrochloric acid, acetic acid, sodium hydroxide, sodium carbonate, ultrapure water, and so on were all analytically pure for this experiment. The apples juice and vitamin B2 tablets were purchased from nearby pharmacies and markets.

**2.1.2 Experimental instruments.** The required instruments for the experiment were Electric Blast Drying Oven (101-2AB, Tianjin), UV-visible spectrophotometer (cary50, Japan), Fluorescence spectrophotometer (F98, Shanghai), Fourier transform infrared spectrometer (WQF-530A, Beijing North Rui Li Analytical Instruments Group Co., Ltd), Electronic analytical balance (SYU-200 Shimadzu, Japan), Desktop high-capacity centrifuge (TG16), Ultrasonic cleaner (KH600KDE, Kunshan) and so on.

### 2.2 Synthesis of Zn/Cl-CQDs

A novel carbon quantum dot (Zn/Cl-CQDs) doped with zinc and chlorine, both metallic and non-metallic elements, was prepared by reacting zinc gluconate and hydrochloric acid in a reaction vessel. In simple terms, 1 g of zinc gluconate was accurately weighed and added to 10 mL of ultrapure water, followed by stirring for 10 min. Then, the pH of the mixture was

adjusted to around 4 using hydrochloric acid solution. The solution was heated in an oven at a temperature of 160 °C for 10 h. Finally, the color of the solution turned orange, confirming the formation of Zn/Cl-CQDs. The final solution was neutralized to an appropriate pH and stored at 4 °C for further use.

### 2.3 Detection and analysis of vitamin B2

**2.3.1 Preparation of vitamin B2 standard solution.** Prepare a standard solution of vitamin B2 with a concentration of 100  $\mu\text{g mL}^{-1}$ . Accurately weigh 10 mg of vitamin B2 (powder) and dissolve it in 100 mL of a 0.2 mol  $\text{L}^{-1}$  acetic acid solution in a 50 mL beaker. Use ultrasound to facilitate the dissolution of vitamin B2, with an ideal ultrasound time of 10–20 min until complete dissolution. Filter the solution using filter paper to obtain the filtrate. Centrifuge the filtrate at 4000 rpm for 10 min to remove any undissolved substances. Transfer the solution to a 100 mL volumetric flask, dilute with a 0.2 mol  $\text{L}^{-1}$  acetic acid solution to the mark, and mix well. Transfer the solution to a light-protected reagent bottle to minimize exposure to light.

**2.3.2 Measurement of fluorescence intensity.** Take 12 groups of 100  $\mu\text{L}$  solutions of CQDs with the same concentration. Adjust the pH of each solution using hydrochloric acid and sodium hydroxide to prepare a pH gradient solution ranging from 1 to 12 with a pH interval of 1. Dilute each solution to 5 mL and measure the fluorescence intensity ( $F_0$ ) of the carbon quantum dots in each solution. Measure the fluorescence intensity ( $F_0$ ) of blank carbon quantum dots corresponding to each pH value. Calculate the corresponding  $F/F_0$  ratio for each pH value and observe the fluorescence quenching effect. Based on the best quenching condition, continue with the spiked recovery experiment.

### 2.4 Spiked recovery experiment

**2.4.1 Preparation of solution and determination of content.** Take 5 vitamin B2 tablets (5 mg each) from Dajin Guangji Pharmaceutical Co., Ltd in Wuxue City, Hubei Province, weigh them, and calculate the average tablet weight. Precisely weigh about 5 mg of finely ground vitamin B2 and dissolve it in 100 mL of a 0.2 mol  $\text{L}^{-1}$  acetic acid solution in a 100 mL beaker. Use ultrasound to facilitate the dissolution of any remaining undissolved vitamin B2 for 10 min. After complete dissolution, filter the solution using filter paper and centrifuge the filtrate at 4000 rpm for 10 min to remove any undissolved substances. Transfer the solution to a 100 mL volumetric flask and dilute with a 0.2 mol  $\text{L}^{-1}$  acetic acid solution to the mark. Mix well and transfer 100  $\mu\text{L}$  of each sample to separate vials. Add 100  $\mu\text{L}$ , 200  $\mu\text{L}$ , 300  $\mu\text{L}$ , *etc.*, of standard solution at different concentrations, as well as 100  $\mu\text{L}$  of carbon quantum dots at different concentrations, and dilute each sample to 5 mL. Measure the fluorescence intensity ( $F$ ) of the sample solution and the blank carbon dot solution ( $F_0$ ). Calculate the concentration of vitamin B2 in the sample solution and the spiked recovery rate based on the standard curve obtained in Section 2.3.



**2.4.2 Extraction and determination of vitamin B2 content in apples.** Weigh 100 g of clean, fresh apples, crush them to obtain a solution, and filter the solution. Centrifuge the filtrate at 4000 rpm for 10 min to remove any undissolved substances. Add 10 mL of a 0.5 mol L<sup>-1</sup> hydrochloric acid solution and transfer the solution to a 100 mL volumetric flask, filling it to the mark. This is because vitamin B2 is relatively stable in an acidic environment and less prone to oxidation and degradation. In addition, Chai Yingying also demonstrated the optimal extraction solvent to be hydrochloric acid when analyzing the influence of different solvents on vitamin extraction. Take 100  $\mu$ L of each sample and add 100  $\mu$ L, 200  $\mu$ L, 300  $\mu$ L, *etc.*, of standard solution at different concentrations, as well as 100  $\mu$ L of carbon quantum dots at different concentrations, and dilute each sample to 5 mL. Measure the fluorescence intensity ( $F$ ) of the sample solution and the blank carbon dot solution ( $F_0$ ). Calculate the concentration of vitamin B2 in the sample solution and the spiked recovery rate based on the standard curve.

## 3. Results and discussion

### 3.1 Characterization of Zn/Cl-CQDs

**3.1.1 TEM characterization.** TEM images could be used to observe the morphology and structure of CQDs, as shown in Fig. 1(a). It was observed that CQDs exhibited monodisperse and uniform spherical distribution. Through statistical software ImageJ analysis, the average size of 100 CQDs particles was 5.0 nm, as shown in Fig. 1(b), indicating that CQDs had very small nanoparticle sizes.

**3.1.2 XRD characterization.** XRD could determine the lattice structure of the prepared Zn/Cl-CQDs. By XRD characterization of solid Zn/Cl-CQDs, the scanning range was set to 10–60°, as shown in Fig. 2, a broad and sharp diffraction peak was observed at  $2\theta = 22.2^\circ$ , indicating that the C atoms of the synthesized Zn/Cl-CQDs exhibited highly disordered state.

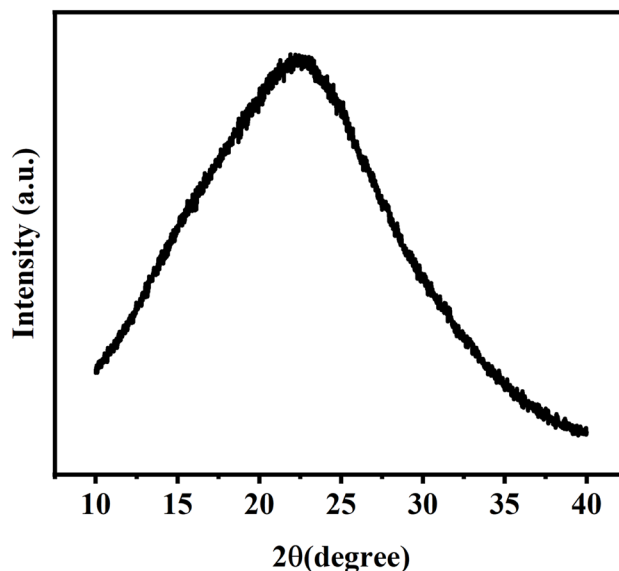


Fig. 2 XRD patterns of Zn/Cl-CQDs.

**3.1.3 FT-IR characterization.** The infrared spectrum of Zn/Cl-CQDs were obtained by FT-IR, as shown in Fig. 3. Based on the FT-IR analysis, a peak was observed around 3300 cm<sup>-1</sup>, indicating the presence of O–H stretching vibration. A broad absorption peak was observed in the range of 1680–1630 cm<sup>-1</sup>, indicating the presence of C=O stretching vibration. A weak absorption peak was observed around 1040 cm<sup>-1</sup>, indicating the presence of C–Cl stretching vibration. Typically, FT-IR spectra revealed the presence of functional groups such as C=O, –COOH and –OH on the surface of CQDs.<sup>31</sup> The CQDs were mainly composed of core–shell structure, the abundant hydroxyl, carbonyl and carboxyl groups on the carbon core confer excellent water solubility. The surface functional groups

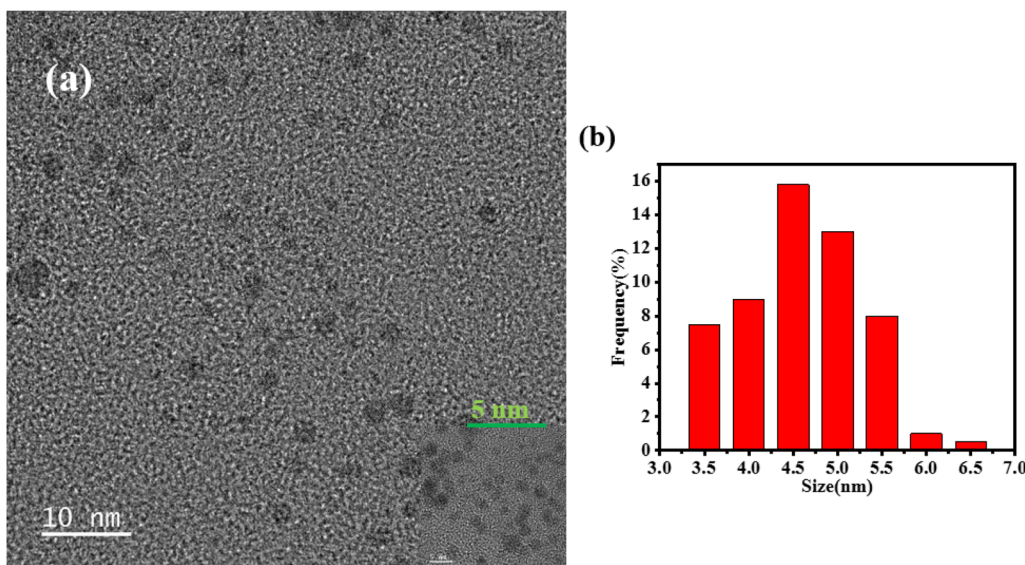


Fig. 1 (a) TEM and (b) particle size distribution maps of CQDs.



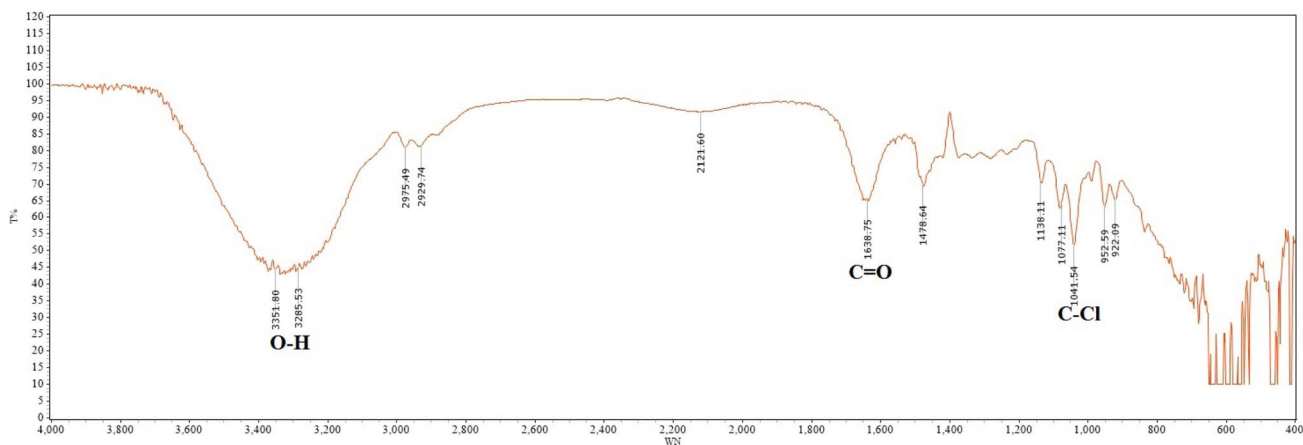


Fig. 3 The FT-IR spectra of CQDs.

enhanced their optical properties, stability, targeting ability, and biocompatibility.

**3.1.4 XPS characterization.** In order to understand the surface element composition and bonding situation of Zn/Cl-CQDs, XPS was used to characterize Zn/Cl-CQDs in this experiment. From Fig. 4, clear peaks of C 1s (285.08 eV), O 1s (531.08 eV), and N 1s (399.08 eV) could be seen, indicating that the sample was mainly composed of C, O and N elements. The appearance of these peaks fully indicated that the surface of Zn/Cl-CQDs was rich in water-soluble functional groups, which was consistent with the characterization results of FT-IR above.

**3.1.5 Optical properties of CQDs.** The optical properties of Zn/Cl-CQDs were studied using fluorescence spectrophotometer. The fluorescence detection was performed, and the obtained fluorescence emission spectrum of the prepared Zn/Cl-CQDs, with an excitation wavelength of 367 nm, as shown in Fig. 5. The maximum emission was observed at wavelength of

734 nm. The figure indicated that the prepared Zn/Cl-CQDs had good fluorescence performance.

### 3.2 Standard curve and linearity

100  $\mu\text{L}$ , 200  $\mu\text{L}$ , 300  $\mu\text{L}$ , 400  $\mu\text{L}$ , and 500  $\mu\text{L}$  of the standard solution were separately diluted to 5 mL, pH was adjusted to 10, and the fluorescence intensity ( $F$ ) values was measured. By calculating the ratio of  $F$  to the fluorescence intensity ( $F_0$ ) of the blank Zn/Cl-CQDs solution, the  $F/F_0$  values was obtained. Plotting  $F/F_0$  as the ordinate and concentration ( $C$ ) as the abscissa, the standard curve shown in Fig. 6 was obtained. Within the concentration range of 0–10  $\mu\text{g mL}^{-1}$ , a good linear relationship was observed between the fluorescence ratio and concentration. The fluorescence intensity of Zn/Cl-CQDs system gradually decreases with the increase of VB2 concentration. The regression equation was  $y = -0.04941x + 0.77976$ , with an  $R^2$  value of 0.9919, with the low detection limit (LOD) of 12.5  $\text{ng mL}^{-1}$ .

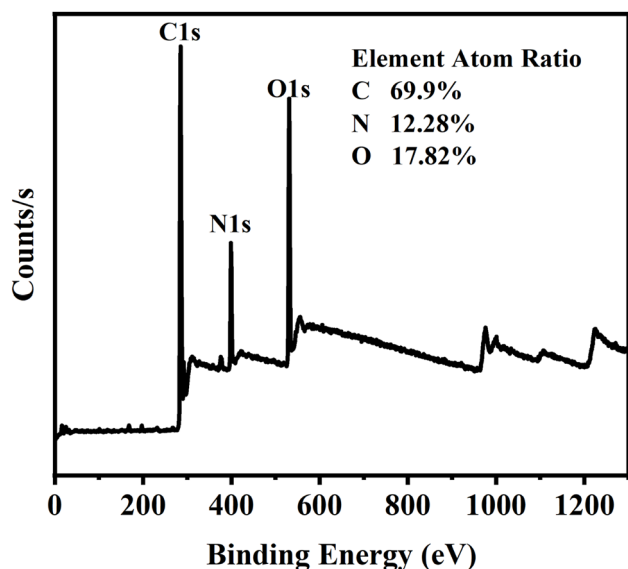


Fig. 4 XPS full spectrum of Zn/Cl-CQDs.

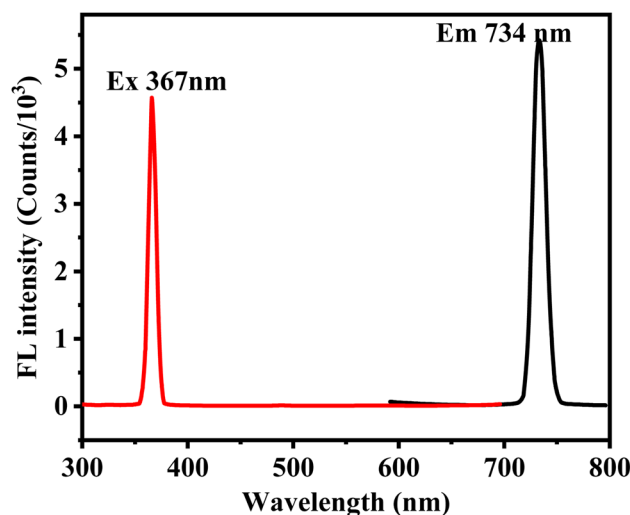


Fig. 5 The optimal fluorescence excitation emission spectrum of CQDs.



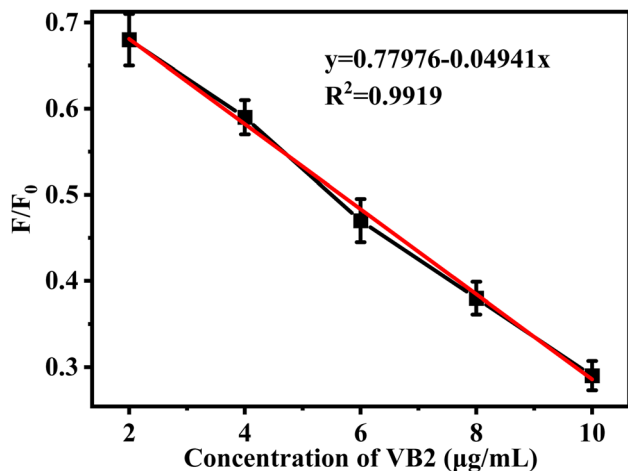


Fig. 6 The standard curve of VB2.

Therefore, Zn/Cl-CQDs system can be used as a fluorescence sensor for detection of VB2 within a concentration range of 0–10  $\mu\text{g mL}^{-1}$ .

### 3.3 Optimization of detection conditions for vitamin B2

**3.3.1 Effect of preparation temperature on the fluorescence intensity of CQDs.** The fluorescence intensity of CQDs prepared at different temperatures (60 °C, 100 °C, 160 °C and 200 °C) were shown in Fig. 7. It was evident that the CQDs prepared at 160 °C exhibited the highest fluorescence intensity. At 160–200 °C, the fluorescence intensity was significantly reduced, indicating that both excessively high and low temperatures could affect the formation of the core of CQDs. Therefore, the prepared CQDs with excellent fluorescence properties, it was necessary to control the appropriate preparation temperature.

**3.3.2 Effect of different pH on fluorescence intensity.** The influence of different pH on the fluorescence intensity of blank

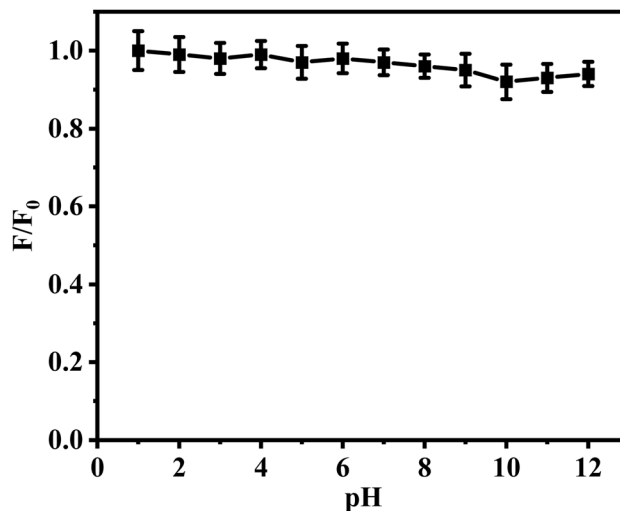


Fig. 8 The effect of different pH values on the fluorescence intensity of CQDs.

CQDs, 12 of 100  $\mu\text{L}$  solutions of CQDs at the same concentration were prepared, and the pH values were adjusted using buffer solutions with different pH values to create pH gradient solutions ranging from pH 1 to 12. The solutions were diluted to 5 mL, and the fluorescence intensity ( $F$ ) of each solution containing CQDs was measured, as shown in Fig. 8. From the graph, it could be seen that the CQDs had excellent stability at different pH values, and was also stable under acidic and alkaline conditions.

Optimization of conditions for detecting VB2, the pH gradient solutions of blank CQDs prepared in the previous step were supplemented with 200  $\mu\text{L}$  solutions of standard vitamin B2 at different concentrations, and the fluorescence intensity was measured and recorded. From Fig. 9, it could be observed that the fluorescence intensity decreased after adding vitamin B2, indicating fluorescence quenching. When the vitamin B2

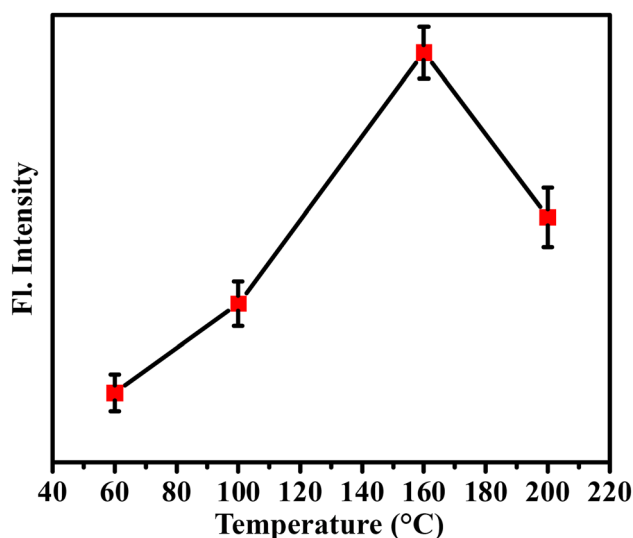


Fig. 7 Optimization of preparation conditions for CQDs.

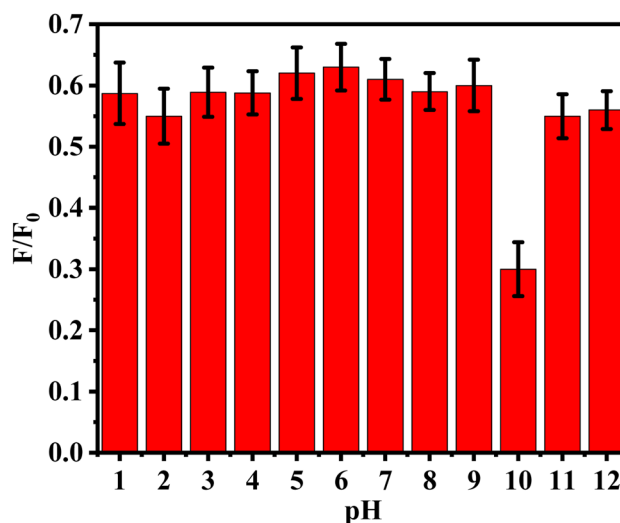


Fig. 9 Optimization of pH conditions for CQDs detection of VB2.

molecules interact with the functional groups on the CQDs surface, their excited-state energy could be transferred through the interaction with the surface functional groups, resulting in quenching of the fluorescence emission of the vitamin B2 molecules. This phenomenon might be attributed to the static quenching mechanism. Notably, at pH 10, the quenching effect was more pronounced compared to other pH conditions.

### 3.3.3 Effect of light exposure on the stability of vitamin B2.

Light exposure is one of the significant factors affecting the stability of vitamin B2. According to relevant literature, vitamin B2 is susceptible to decomposition and inactivation under strong light, leading to a decrease in its content. Weaker light exposure has a lesser impact. To maintain the stability of vitamin B2, it is advisable to store it under dark conditions or in opaque containers, avoiding exposure to strong light sources such as sunlight.

### 3.3.4 Effect of ultrasound time on detecting vitamin B2.

To enhance the dissolution of vitamin B2, ultrasonication was employed in this experiment. The ultrasound time was an important factor influencing the extraction yield of vitamin B2. Generally, longer ultrasound time resulted in higher extraction yield of vitamin B2. However, the experiments had shown that excessively long ultrasound time could lead to the decomposition and loss of vitamin B2, thereby affecting the extraction efficiency. During ultrasonic extraction of vitamin B2, the highest extraction yield was achieved when the ultrasound time was around 10–20 min. When the ultrasound time exceeded 20 min, the extraction yield of vitamin B2 began to decrease. This was because prolonged ultrasound time could cause the decomposition and loss of vitamin B2, as well as the precipitation and denaturation of other organic substances, thereby affecting the extraction efficiency. Therefore, it was necessary to choose an appropriate ultrasound time based on the characteristics of the sample and experimental conditions to obtain optimal extraction efficiency. Additionally, it was important to exercise caution as excessively long ultrasound time might have detrimental effects on the sample and should be appropriately controlled.

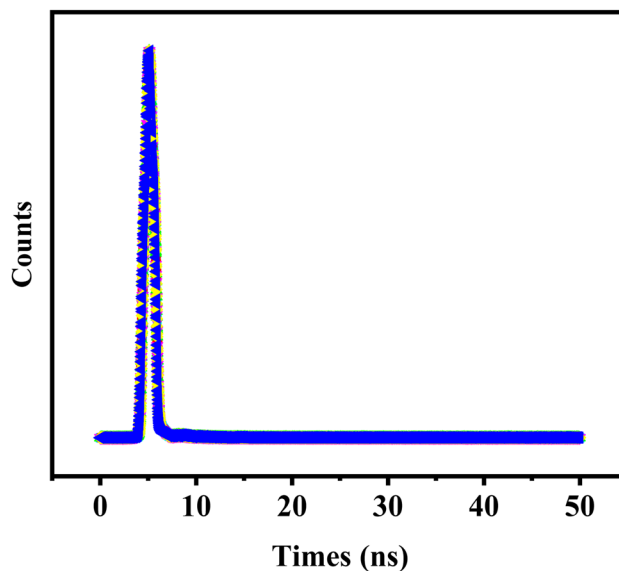
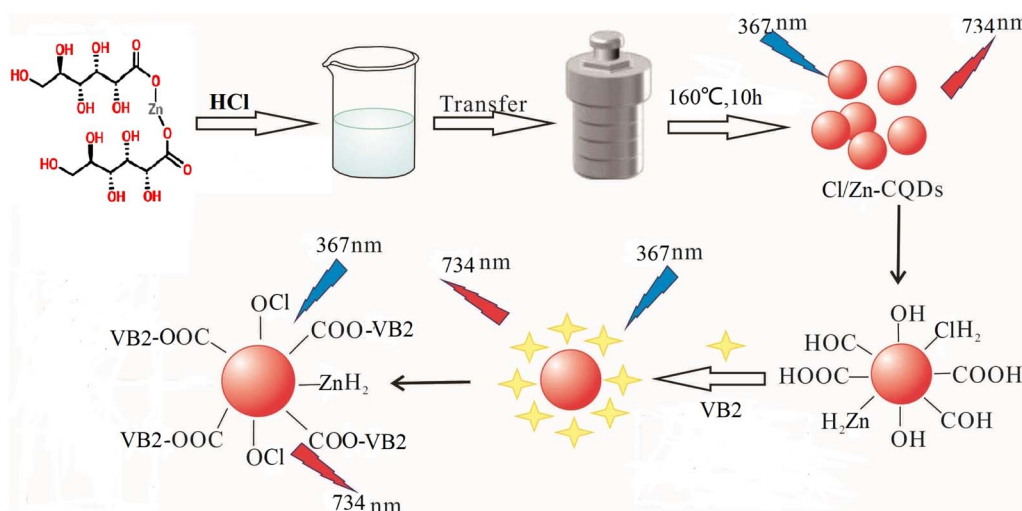


Fig. 10 Fluorescence decay curves of Zn/Cl-CQDs, Zn/Cl-CQDs + VB2 (0–50  $\mu\text{g mL}^{-1}$ ).

### 3.4 The response mechanism

Based on the FT-IR characterization of Zn/Cl-CQDs and the structural diagram of VB2 (Fig. 3), it can be concluded that, the reason may be due to the binding between VB2 and Zn/Cl-CQDs during the reaction process. The characterization by Zn/Cl-CQDs indicates that the surface of Zn/Cl-CQDs contains hydrophilic functional groups ( $-\text{OH}$  and  $-\text{COOH}$ ), while VB2 also contains water-soluble functional groups ( $-\text{OH}$ ,  $-\text{CO}-\text{NH}-$ ). These functional groups can couple through hydrogen bonds and produce aggregation effects, leading to shift in the absorption peak of the system and quenching of fluorescence, the possible reaction structure diagram is shown in Scheme 1.

The fluorescence lifetime of Zn/Cl-CQDs before and after the reaction with VB2 is also measured in the experiment, as shown in Fig. 10. The average fluorescence lifetime is calculated by the



Scheme 1 The synthesis route of Zn/Cl-CQDs and the schematic diagram for detecting VB2.



Table 1 Actual samples spiked recovery rates ( $n = 3$ )

Actual sample	Measurement ( $\mu\text{g mL}^{-1}$ )	Spiked ( $\mu\text{g mL}^{-1}$ )	Detected ( $\mu\text{g mL}^{-1}$ )	Recovery rate (%)	Average recovery (%)	RSD%
Vitamin B2 tablets	1.7	2.00	3.65	97.5%	98.2%	1.8
		4.00	5.79	101%		2.0
		6.00	7.52	96.2%		2.1
Apple juice	1.05	2.00	3.01	98.0%	100.6%	3.1
		4.00	5.22	104.2%		2.5
		6.00	7.02	99.5%		3.3

formula<sup>32</sup> and its weighted average value shows that the average lifetime of Zn/Cl-CQDs is 5.152 ns, and the average lifetime after the reaction between Zn/Cl-CQDs and VB2 is 5.148 ns. The values remain basically unchanged, indicating that the reaction process between Zn/Cl-CQDs and VB2 belongs to static quenching.

### 3.5 Analysis of real samples

Based on the results of the spiking experiments, the data presented in Table 1 were obtained. The average recovery rates for the vitamin B2 tablets and apple juice were found to be 98.2% and 100.6%, respectively. RSD% were 1.8–2.1% and 2.5–3.3%, which indicated that this method had high sensitivity and accuracy. Therefore, this method could be well applied to the detection of VB2 concentration in actual samples.

## 4. Conclusion

This study presented the synthesis of a novel carbon quantum dots (Zn/Cl-CQDs) doped with zinc and chlorine, and their application in the detection of vitamin B2. Vitamin B2 is an important nutrient with significant roles in human health. Traditional methods for vitamin B2 detection suffer from long detection times and complex procedures. Carbon quantum dots, with their advantages of rapid response, high sensitivity, and good selectivity, offer a promising approach for the detection of vitamin B2.

The properties of the synthesized carbon quantum dots were analyzed and discussed, including the fluorescence intensity variation at different pH values and temperatures, providing a theoretical basis for the preparation, storage, and development of carbon quantum dots. The extraction conditions and stability of Vitamin B2 were also analyzed and discussed, creating favorable conditions for the detection and quantification of Vitamin B2. Finally, the average recovery rates of Vitamin B2 tablets and Vitamin B2-rich apple juice using Zn/Cl-CQDs as the detection method were 98.2% and 100.6%, respectively.

## Data availability

All data generated or analysed during this study are included in this published article.

## Conflicts of interest

All authors declare no conflict of interest.

## Acknowledgements

This work was supported by Bijie City Science and Technology Bureau Joint Fund Project ((2023)46), Guizhou Coal Chemical Engineering Collaborative Innovation Center and Bijie Coal Phosphorus Chemical Engineering Technology Center (No. (2014)08 and (2015)01).

## References

- 1 S. Ohkuma and B. Poole, Fluorescence probe measurement of the intralysosomal pH in living cells and the perturbation of pH by various agents, *Proc. Natl. Acad. Sci. U. S. A.*, 1978, 75(7), 3327–3331, DOI: [10.1073/pnas.75.7.3327](https://doi.org/10.1073/pnas.75.7.3327).
- 2 A. P. Senft, T. P. Dalton and H. G. Shertz, Determining glutathione and glutathione disulfide using the fluorescence probe o-phthalaldehyde, *Anal. Biochem.*, 2000, 280(1), 80–86, DOI: [10.1006/abio.2000.4498](https://doi.org/10.1006/abio.2000.4498).
- 3 Y. Koide, Y. Urano, K. Hanaoka, *et al.*, Development of an Si-Rhodamine-Based Far-Red to Near-Infrared Fluorescence Probe Selective for Hypochlorous Acid and Its Applications for Biological Imaging, *J. Am. Chem. Soc.*, 2011, 133(15), 5680–5682, DOI: [10.1021/ja111470n](https://doi.org/10.1021/ja111470n).
- 4 P. Lyon, V. Strippoli, B. Fang, *et al.*, B Vitamins and One-Carbon Metabolism: Implications in Human Health and Disease, *Nutrients*, 2020, 12(9), 2867.
- 5 Z. Zhang, J. Xu, Y. Wen, *et al.*, A highly-sensitive VB2 electrochemical sensor based on one-step co-electrodeposited molecularly imprinted WS<sub>2</sub>-PEDOT film supported on graphene oxide-SWCNTs nanocomposite, *Mater. Sci. Eng. C*, 2018, 92, 77–87.
- 6 S. A. És, P. Silva, C. L. Jost, *et al.*, Electrochemical sensor based on bismuth-film electrode for voltammetric studies on vitamin B2 (riboflavin), *Sens. Actuators, B*, 2015, 209, 423–430.
- 7 J. Jia, W. J. Lu, S. Cui, C. Dong and S. M. N. Shuang, Cl-doped carbon dots for fluorescence and colorimetric dual-mode detection of water in tetrahydrofuran and development of a paper-based sensor, *Microchim. Acta*, 2021, 188, 324.
- 8 P. F. Fan, C. Liu, C. C. Hu, *et al.*, Orange-emissive N, S-codoped carbon dots for label-free and sensitive fluorescence assay of vitamin B12, *New J. Chem.*, 2022, 46(2), 877–882.
- 9 F. F. Du, Z. Cheng, G. H. Wang, *et al.*, Carbon Nanodots as a Multifunctional Fluorescent Sensing Platform for



- Ratiometric Determination of Vitamin B2 and “Turn-Off” Detection of pH, *J. Agric. Food Chem.*, 2021, **69**(9), 2836–2844.
- 10 P. T. Kumar, K. Shrivastava, A. Patle, *et al.*, Simultaneous determination of B1, B3, B6 and C vitamins in green leafy vegetables using reverse phase-high performance liquid chromatography, *Microchem. J.*, 2022, **176**, 107249.
  - 11 F. Tezcan and F. B. Erim, Determination of Vitamin B2 Content in Black, Green, Sage, and Rosemary Tea Infusions by Capillary Electrophoresis with Laser-Induced Fluorescence Detection, *Beverages*, 2018, **4**(4), 86, DOI: [10.3390/beverages4040086](https://doi.org/10.3390/beverages4040086).
  - 12 L. Zeng, W. Jiang, L. Liu, *et al.*, Development of ic-ELISA and lateral-flow immunochromatographic strip for detection of vitamin B2 in an energy drink and vitamin tablets, *Food Agric. Immunol.*, 2017, (8), 1–12, DOI: [10.1080/09540105.2017.1360257](https://doi.org/10.1080/09540105.2017.1360257).
  - 13 Q. Liu, J. Wang and B. J. Boyd, Peptide-based biosensors, *Talanta*, 2015, **136**, 114–127.
  - 14 H. Yu, K. Ryu, J. Park, S. Subedi and K. H. Lee, Design and synthesis of fluorescent peptide-based probes with aggregation-induced emission characteristic for detecting  $\text{CH}_3\text{Hg}^+$  and  $\text{Hg}^{2+}$  in aqueous environment: Tuning fluorescent detection for  $\text{CH}_3\text{Hg}^+$  by replacing peptide receptors, *Dyes Pigm.*, 2022, **204**, 110461.
  - 15 P. Wang, L. Sun, J. Wu, X. Yang, P. Lin and M. Wang, A dual-functional colorimetric and fluorescent peptide-based probe for sequential detection of  $\text{Cu}^{2+}$  and  $\text{S}^{2-}$  in 100% aqueous buffered solutions and living cells, *J. Hazard. Mater.*, 2021, **407**, 124388.
  - 16 Y. An, W. Chang, W. Wang, H. Wu, K. Pu, A. Wu, Z. Qin, Y. Tao, Z. Yue, P. Wang and Z. Wang, A novel tetrapeptide fluorescence sensor for early diagnosis of prostate cancer based on imaging  $\text{Zn}^{2+}$  in healthy *versus* cancerous cells, *J. Adv. Res.*, 2020, **24**, 363–370.
  - 17 J. Lv, W. Yang and Y. Miao, Preparation of N-doped carbon dots and application to enhanced photosynthesis, *Spectrochim. Acta, Part A*, 2023, **297**, 122763, DOI: [10.1016/J.SAA.2023.122763](https://doi.org/10.1016/J.SAA.2023.122763).
  - 18 M. Amarnath and C. Balalakshmi, Preparation of N, S-doped blue emission carbon dots for dual-mode glucose detection with live cell applications, *Chem. Pap.*, 2023, **77**(8), 4193–4199, DOI: [10.1007/s11696-023-02769-5](https://doi.org/10.1007/s11696-023-02769-5).
  - 19 L. Xiao, Q. Du, Y. Huang, *et al.*, Rapid synthesis of sulfur nanodots by one-step hydrothermal reaction for luminescence-based applications, *ACS Appl. Nano Mater.*, 2019, **2**, 6622–6628.
  - 20 C. Zhang, P. Zhang, X. Ji, *et al.*, Ultrasonication-promoted synthesis of luminescent sulfur nano-dots for cellular imaging applications, *Chem. Commun.*, 2019, **55**, 13004–13007.
  - 21 R. Cai, L. Xiao, M. X. Liu, *et al.*, Recent advances in functional carbon quantum dots for antitumour, *Int. J. Nanomed.*, 2021, **16**, 7195.
  - 22 Y. X. Hou, Q. J. Lu, J. H. Deng, *et al.*, One-pot electrochemical synthesis of functionalized fluorescent carbon dots and their selective sensing for mercury ion, *Anal. Chim. Acta*, 2015, **866**, 69–74.
  - 23 S. Javanbakht, M. T. Nazeri, A. Shaabani, *et al.*, Green one-pot synthesis of multicomponent-crosslinked carboxymethyl cellulose as a safe carrier for the gentamicin oral delivery, *Int. J. Biol. Macromol.*, 2020, **164**, 2873–2880.
  - 24 Y. P. Hao, R. H. Li, Y. X. Liu, *et al.*, The on-off-on Fluorescence Sensor of Hollow Carbon Dots for Detecting  $\text{Hg}^{2+}$  and Ascorbic Acid, *J. Fluoresc.*, 2023, **33**(2), 459–469.
  - 25 Y. Huang, J. Ren and X. Qu, Nanozymes: Classification, catalytic mechanisms, activity regulation, and applications, *Chem. Rev.*, 2019, **119**(6), 4357–4412.
  - 26 H. V. Tran, T. V. Nguyen, N. D. Nguyen, *et al.*, A nanocomposite prepared from FeOOH and N-doped carbon nanosheets as a peroxidase mimic, and its application to enzymatic sensing of glucose in human urine, *Mikrochim. Acta*, 2018, **185**(5), 270.
  - 27 M. S. Kim, J. Lee, H. S. Kim, *et al.*, Heme cofactor-resembling Fe-N single site embedded graphene as nanozymes to selectively detect  $\text{H}_2\text{O}_2$  with high sensitivity, *Adv. Funct. Mater.*, 2020, **30**(1), 1905410.
  - 28 W. Liu, L. Chu, C. Zhang, *et al.*, Hemin-assisted synthesis of peroxidase-like Fe-N-C nanozymes for detection of ascorbic acid-generating bio-enzymes, *Chem. Eng. J.*, 2021, **415**, 128876.
  - 29 Y. Guo and W. Zhao, Hydrothermal synthesis of highly fluorescent nitrogen-doped carbon quantum dots with good biocompatibility and the application for sensing ellagic acid, *Spectrochim. Acta, Part A*, 2020, **240**, 118580.
  - 30 M. Preethi, R. Murugan, C. Viswanathan and N. Ponpandian, Potato starch derived n-doped carbon quantum dots as a fluorescent sensing tool for ascorbic acid, *J. Photochem. Photobiol., A*, 2022, **431**, 114009.
  - 31 X. X. Yang, F. C. Cui, R. Ren, *et al.*, Red-Emissive Carbon Dots for “Switch-On” Dual Function Sensing Platform Rapid Detection of Ferric Ions and L-Cysteine in Living Cells, *ACS Omega*, 2019, **4**(7), 12575–12583.
  - 32 Y. Tu, Z. Liu and L. Jiang, Green ratiometric fluorescent dual-mode nanosensor for highly selective and sensitive detection of new coccine in food, *Dyes Pigm.*, 2023, **210**, 111024–111027.

